Science of the Total Environment xxx (xxxx) xxx

Contents lists available at ScienceDirect

Science of the Total Environment

journal homepage: www.elsevier.com/locate/scitotenv

Influence of temperature and pH on phosphate removal efficiency of different sorbents used in lake restoration

Li Kang *, Maíra Mucci, Miquel Lürling

Aquatic Ecology & Water Quality Management Group, Department of Environmental Sciences, Wageningen University, P.O. Box 47, 6700 AA Wageningen, the Netherlands

HIGHLIGHTS

- Modified bentonite, zeolite and aluminium salts bound phosphate (SRP).
- Langmuir isotherm model fitted the phosphate binding process adequately.
- Phosphate binding onto P sorbents (PS) was exothermic and spontaneous.
- Effects of pH and temperature on SRP binding performance differed among PS.

GRAPHICAL ABSTRACT

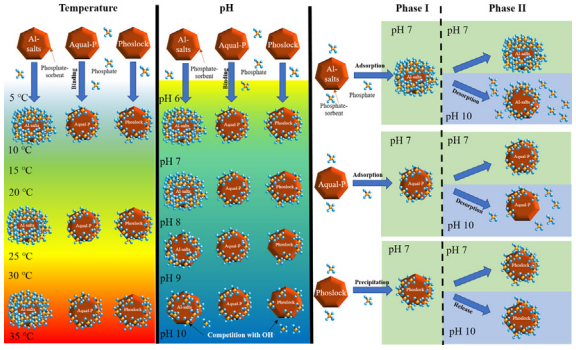

ARTICLE INFO

Article history:
Received 10 August 2021
Received in revised form 2 November 2021
Accepted 2 November 2021
Available online xxxx

Editor: Ouyang Wei

Keywords:
Phosphorus removal
Phoslock
Aqual-P
Alum
Lake restoration
Eutrophication

ABSTRACT

Phosphorus sorbents (PS) are viewed as a powerful tool to manage eutrophication. Here, we tested three commercially available PS - lanthanum-modified bentonite (LMB), aluminium-modified zeolite (AMZ) and aluminium salts (Al) on their capacity to chemically inactivate soluble reactive phosphorus (SRP) at six different temperatures (5 to 35 °C) and five pH values (6 to 10). We also evaluated if the SRP bound at a neutral pH would be released if pH increases to pH 10. Results showed that temperature affected the SRP binding behavior differently for each PS. For instance, the highest SRP binding capacities of LMB, AMZ and Al were 14.0, 29.9 and 251.1 mg P g^{-1} at 30 °C, 35 °C and 30 °C, respectively; and the lowest was at 35 °C for LMB, 25 °C for AMZ and 20 °C for Al (6.3, 4.0 and 205.2 mg P g^{-1}, respectively). The pH also affected the SRP binding differently. When pH increased from pH 6 to pH 10, LMB and Al decreased their binding capacity from 10.0 to 4.9 and from 571.7 mg P g^{-1} to 21.3 mg P g^{-1}, respectively. The SRP adsorption capacity of AMZ was similar at pH 7 and 10 (6.3 and 6.2 mg P g^{-1}). We observed that in high pH, LMB did not release the SRP precipitated. In contrast, AMZ and Al desorbed around 39%, and 71% of the SRP adsorbed when pH changed from 7 to 10. Abiotic factors such as pH should be considered when selecting the most promising material in lake restoration.

1. Introduction

Anthropogenic activities have led to significant water quality deterioration in lakes worldwide, in which eutrophication is the most prevalent water quality issue (OECD, 2017; Smith and Schindler, 2009). The most hazardous effect of eutrophication is the extensive biomass of phytoplankton, especially cyanobacterial blooms. These blooms increase water turbidity, shade submerged aquatic plants, smother aquatic animals due to nighttime hypoxia/anoxia, and present a danger to wildlife, pets and humans from the toxins several cyanobacteria species may produce (Paerl and Paul, 2012). Consequently, eutrophication impairs important ecosystem services. In Europe, 57% of the rivers and 44% of the lakes failed to meet the 2015 requirements set by the

* Corresponding author.
E-mail address: li.kang@wur.nl (L. Kang).

https://doi.org/10.1016/j.scitotenv.2021.151489

European Water Framework Directive (WFD) (Poikane et al., 2019). In the Netherlands, between 2011 and 2013, 60% of the WFD waterbodies were assessed as eutrophic (Fraters et al., 2017), and in a recent survey, still, 50% of the WFD waterbodies failed to meet the nitrogen (N) standard or the phosphorus (P) standard (van Galen et al., 2020). In China, 57.5% of freshwater lakes have become eutrophic or hypertrophic (Jin et al., 2005). Such widespread eutrophication affects important services that freshwater ecosystems provide to society, increasing the financial burden and causing substantial economic losses (Sanseverino et al., 2016). The estimated annual cost of freshwater eutrophication in OECD countries is approximately $1100 billion (OECD, 2017). Thus, it is key to manage eutrophication and mitigate its negative effects.

Generally, reducing external nutrient input is crucial to achieve sustainable restoration of eutrophic lakes and to prevent harmful cyanobacterial blooms (Hamilton et al., 2016; Paerl, 2014; Paerl et al., 2016). In most OECD countries, point source nutrient pollution has been tackled, while diffuse nutrient pollution remains a challenge (OECD, 2017). In addition, nutrients legacies from the past, accumulated and periodically recycled from the sediment, may hamper rapid recovery after external, point-source nutrient control (Fastner et al., 2016; Søndergaard et al., 2013). This internal nutrient load has prompted research into methods that effectively mitigate nutrient release from sediments and includes a plethora of techniques ranging from sediment removal, hypolimnetic water withdrawal, and oxygenation to chemical treatments (Lürling et al., 2020).

In particular, P-sorbents (PS) are promising candidates to reduce P as an important building block for cyanobacterial biomass (Douglas et al., 2016; Lürling et al., 2016; Spears et al., 2013). Reducing P sufficiently with PS may minimize the effects of eutrophication (Lürling and van Oosterhout, 2013). The use of PS to manipulate biogeochemical processes is known as geo-engineering, which has been recognized as a powerful tool to manage eutrophication and control cyanobacteria blooms in water bodies where the internal load is high (Lürling et al., 2020). Those PS must be effective, easy to manufacture and use, relatively inexpensive and safe.

The most commonly used PS is aluminium salts, such as aluminium sulphate (alum), due to their wide application range, relatively low price and ubiquitous availability. Aluminium sulphate is a white crystalline solid and it is commonly composed of two atoms of aluminium, 3 sulfur and 12 atoms of oxygen (Dionisio et al., 2018). Once added, Al salts will form flocks ($Al(OH)_3$) adsorbing available phosphate (SRP) and, due to their coagulating properties will also instantaneously improve water transparency (Cooke et al., 2005; Gibbs and Hickey, 2018; Lürling et al., 2020). Alum is often applied with a buffer such as sodium aluminate to avoid large pH changes. A ballast compound can also be added together with alum to enhance the settlement of Al-flocs, ensuring that flocs and cyanobacteria end up on the sediment. The ballast can be natural soils (Noyma et al., 2016) or a solid phase P sorbent (SPS), but SPS compounds can also be used alone (Lürling et al., 2020). The most abundantly used SPS is Phoslock®, a lanthanum modified bentonite (LMB) (Copetti et al., 2016; Douglas, 2002) that can effectively precipitate the SRP from the water column and intercept and capture SRP released from the sediments (Douglas et al., 2016). Phoslock is manufactured via an ion exchange process whereby lanthanum ions displace sodium ions within the bentonite matrix (Fig. S1). The bentonite structure contains two basic blocks, i.e. the aluminium octahedral sheets and silica tetrahedral sheets and due its high ions exchange capacity the cations (e.g. Na^+) between the blocks can be easily replaced by lanthanum (Hebbar et al., 2014; Ross and Shannon, 1926). The removal of SRP by LMB is attributed to 5% lanthanum (La), which binds phosphate molecules and forms rhabdophane ($LaPO_4{\cdot}nH_2O$), a mineral with highly stable low solubility ($K_{sp} = 10^{-24.7}$ to $10^{-25.7}$ $mol^2\ L^{-2}$) (Johannesson and Lyons, 1994). Thus, when La in LMB comes in contact with phosphate, the chemical bonding leads to precipitation of an insoluble mineral. Another promising SPS is Aqual-P™, an aluminium modified zeolite (AMZ). Zeolites are natural and synthetic silicoaluminates characterized by a microporous crystal structure which is based on two main structural units constituted by silicon or aluminium atoms or other elements bonded to four oxygen atoms, and oxygen being bonded to two tetrahedral atoms (Busca, 2014). AMZ is an aluminium-based P-inactivator that uses zeolite as an aluminium carrier and does not require buffering to avoid acidification of the lake water. AMZ differs from Al in both physical and chemical properties, with a higher density and a lower weight-specific P-binding capacity (Gibbs and Özkundakci, 2011). AMZ was tested and applied as a sediment capping agent in Lake Okaro, New Zealand (Gibbs and Hickey, 2018) and so far it is the only known commercially available sediment capping agent that inactivates both P and N (Gibbs and Özkundakci, 2011). Hence, Al and AMZ chemically inactivate phosphorus via adsorption and LMB via precipitation (Fig. S1).

The SRP binding efficacy of PS may depend on the prevailing conditions related to the binding mechanism, such as pH, redox state and temperature (Lürling et al., 2014; Mucci et al., 2018; Noyma et al., 2016). For instance, increasing temperature improves the bond energy of phosphorus binding in the soil, increasing the rate of P transfer to strongly bound forms. Thus P retention ability is enhanced at a higher temperature (Reddy and DeLaune, 2008). It is common knowledge that water temperature changes temporarily and daily with the air temperature. As the average global temperature has risen by about 0.8 °C since 1980, warming waters may also stimulate P release from the sediment, likely as a response to the lower oxygen concentrations and thus iron-bound P release increases from the sediment as well as enhanced mineralization of organic matter (Jeppesen et al., 2009). Similarly, pH may influence the efficacy of PS. The ligand exchange between SRP and OH^- can desorb SRP at high pH values because the ligands of OH^- in solution may replace the complexed HPO_4^{2-} or $H_2PO_4^-$ ions (Du et al., 2016). Each PS may act differently under different pH values. For instance, LMB showed excellent SRP removal when tested in the pH range of 6 to 9 (Li et al., 2019; Mucci et al., 2018; Ross et al., 2008). The maximum adsorption capacity of AMZ was highest at pH 9 (Mucci et al., 2018), while the optimum SRP removal of alum occurs between pH 5 to 7 (Georgantas and Grigoropoulou, 2007).

Although water bodies have different water temperatures within the season, which influence the system, none or a few studies have considered a realistic temperature range as a possible factor influencing PS binding efficiency (Georgantas and Grigoropoulou, 2007). Thus, here we determined the SRP binding capacity of LMB, AMZ and Al at six temperatures (from 5 to 35 °C) to test the hypothesis that more SRP will be immobilized at warmer temperatures. Moreover, in a previous study (Mucci et al., 2018), both LMB and AMZ were tested in the pH range 6 to 9; however, depending on their acid-neutralizing capacity, pH values of 10 can be reached in shallow lakes (Kragh and Sand-Jensen, 2018). Hence, the present study elaborated on this, including pH 10. We tested the hypothesis that high pH will hamper the SRP binding capacity in all the PS tested due to competition with hydroxyl ions for binding sites (Li et al., 2019). In natural waters, pH can change within different seasons; however, little is known about SRP desorption caused by pH changes. Thus we also evaluated if a change in pH, from 7 to 10, would cause SRP release, testing the hypothesis that more SRP will be desorbed at a higher pH.

2. Methods

2.1. P sorbents

Three common P sorbents were selected: 1) La-modified bentonite Phoslock® (LMB), 2) Al-modified zeolite Aqual-P™ (AMZ), and 3) aluminium (Al) as combined aluminium sulphate (alum) and sodium aluminate. The La-modified bentonite Phoslock® (LMB), which size is 0.2– 5 mm, was obtained from Phoslock® Europe GmbH (Zug, Switzerland). Before use, Phoslock was ground and sieved through a 0.5 mm mesh. Five different batches of LMB ("Open Luchtmuseum",

and batches no. 20050922, no. 20050929, no. 20060727, no. 20060708) were destructed with a nitric acid/hydrochloric acid mixture (Aqua Regia) in the Chemical Biological Soil Laboratory of the Department of Soil Sciences (Wageningen University) and subsequently analyzed on Hg (AAS-cold vapour), Al, Fe, Mn, P, Zn (ICP-AES, IRIS Intrepid II; Thermo Electron Corporation, Franklin, MA, USA), and As, Cd, Cr, Cu, La, Pb (ICP-MS, Thermo Element 2; Thermo Fisher Scientific). LMB contains no detectable Hg (all below LOD <0.03 mg kg^{-1}), 49,707 (1925) mg Al kg^{-1}, 43,656 (1568) mg La kg^{-1},17,354 (660) mg Fe kg^{-1}, 161 (30) mg Mn kg^{-1}, 211 (44) mg P kg^{-1}, 44 (3) mg Zn kg^{-1}, 1.3 (0.3) mg As kg^{-1}, 0.12 (0.01) mg Cd kg^{-1}, 12.1 (0.7) mg Cr kg^{-1}, 6.6 (0.6) mg Cu kg^{-1}, and 18 (2) mg Pb kg^{-1}. The Al-modified zeolite Aqual-P™ (AMZ), which size is < 0.5 mm, was obtained from Blue Pacific Minerals (Tokoroa, New Zealand), AMZ composition was analyzed by ICP-OES (Thermo iCAP 6500 DV; Thermo Fisher Scientific) at the Chemical Biological Soil Laboratory of the Department of Soil Sciences (Wageningen University). Before using ICP-OES, AMZ were digested using a nitric acid/hydrochloric acid mixture (= Aqua Regia). AMZ contained 26,458 mg Al kg^{-1}, 10,131 mg Fe kg^{-1}, 15,290 mg Na kg^{-1}, 8484 mg K kg^{-1}, 8200 mg Ca kg^{-1}, 2503 mg Mg kg^{-1}, 2295 mg S kg^{-1}, 1081 mg P kg^{-1}, 629 mg Mn kg^{-1}, 63 mg Zn kg^{-1}, 4 mg Cr kg^{-1}, 4 mg Cu kg^{-1}, and 1.9 mg Ni kg^{-1}. We combined two aluminium salts (Al), aluminium sulphate (alum) and sodium aluminate, as a buffer, which is a common procedure in lake restoration (e.g. Cooke et al., 2005; Smeltzer et al., 1999). Alum (aluminium sulphate, $Al_2(SO_4)_3 \bullet nH_2O$, sulfuric acid and aluminium salt 3:2, tetradecahydrate 80%–100%, size is below 5 mm) was obtained from Kemira (Helsinki, Finland), and sodium aluminate (Al_2O_3: 50–56%, Na_2O: 37–45%, size is below 0.5 mm) was acquired from Sigma-Aldrich (Darmstadt, Germany). Both alum and sodium aluminate were obtained as solid materials.

2.2. Effect of temperature on SRP binding capacity

Eight different phosphate (SRP) solutions (0, 5, 10, 20, 40, 80, 120 and 140 mg P L^{-1}) were prepared by dissolving KH_2PO_4 in nanopure water. The SRP solution (50 mL) was transferred into 50 mL screw-cap centrifuge tubes and pH adjusted to pH 7 by adding HCl (0.1 M) or NaOH (0.1 M). Samples of the initial P solutions were stored at −20 °C for further SRP analysis. To each of the eight different P solutions, 80 mg of AMZ or LMB were added. A stock solution from alum and sodium aluminate (both concentrations are 3158 mg Al L^{-1}) was prepared, and their addition was intercalated to avoid large pH change while adding the aluminium salts. pH was measured whenever a proportion of Al (alum or sodium aluminate) was added to the tubes. In the end, a total of 6.32 mg Al, half from alum and half from sodium aluminate, was added to each of the eight P solutions (Table S1). Once the materials were added, the tubes were placed for 24 h in an incubator under different temperatures (5, 10, 15, 20, 25, 30 and 35 °C) and continuously mixed (180 rpm) to keep the PS suspended. The experiment was run in triplicate. After 24 h, the tubes were centrifuged for 5 min at 2500 rpm (Heraeus sepatech centrifuge), and the supernatant was filtered through unit filters (Aqua 30/0.45 CA, Whatman, Germany). SRP concentrations of the filtrates and the initial solutions were determined using a Skalar SAN^+ segmented flow analyzer (Detection limit was 10 μg P L^{-1}), which follows the Dutch standard NEN 6663 (NNI, 1986). The final pH of the supernatant was also measured using a WTW pH meter equipped with a Sentix 61 electrode.

2.3. Effect of pH on SRP binding capacity

The maximum SRP binding capacity of the three PS was measured at pH 6, 7, 8, 9 and 10, following the same method described in Section 2.2. The pH of the SRP solutions with LMB or AMZ was adjusted with HCl (0.1 M) or NaOH (0.1 M) to attain the desired pH. In the Al experiment, pH was adjusted by changing the alum and sodium aluminate ratio (Table S1). After the pH adjustment and material addition, the tubes were shaken (180 rpm) for 24 h at 20 °C. After 24 h, SRP and pH were measured as previously described.

2.4. Effect of changes in pH on SRP release

A SRP binding experiment, as described in Section 2.2, was conducted for each of the PS at pH 7 (Phase I). Per PS (LMB, AMZ and Al), 6 replicates were used for each of the eight SRP concentrations (0, 5, 10, 20, 40, 80, 120 and 140 mg P L^{-1}), yielding 48 experimental units per PS. The test tubes were incubated at 20 °C and constantly shaken (180 rpm). After 24 h, from each tube 15 mL solution was collected, filtered through unit filters and stored in the freezer for further SRP analysis, as described previously. Subsequently, for each compound, the six tubes per SRP concentration were split into two series of three replicates. In one series, the pH was changed to pH 10 by adding NaOH (0.1 M), and the conductivity was adjusted by using NaCl to make sure all the incubations had similar conductivity, while the second series remained at pH 7 (Phase II). The tubes were incubated again and after another 24 h, the pH was measured, tubes were centrifuged, and 30 mL solution was collected and analyzed for SRP concentration as previously described. SRP release was calculated based on the difference between maximum SRP concentrations of Phase I and Phase II.

2.5. Data analysis

To calculate the maximum SRP binding capacity, the Langmuir and Freundlich models were used. The amount of SRP bound to PS at equilibrium Q_e (mg P g^{-1}) was calculated using Eq. (1) based on the initial concentration of SRP in solution C_0 (mg P L^{-1}), the SRP concentration at equilibrium C_e (mg P L^{-1}) from the adsorption/precipitation experiment, the volume of SRP solution V (L) and the weight of PS M (g) (Jalali and Peikam, 2013):

$$Q_e = \frac{(C_0 - C_e)V}{M} \quad (1)$$

The Langmuir isotherm was expressed in Eqs. (2) and (3). Maximum binding capacity Q_m (mg P g^{-1}), the Langmuir adsorption/precipitation constant K_L (L mg^{-1}) was calculated using Eq. (2) based on plotting versus C_e (Langmuir, 1918; Mucci et al., 2018):

$$\frac{C_e}{Q_e} = \frac{1}{Q_m K_L} + \frac{C_e}{Q_m} \quad (2)$$

In order to evaluate the reaction rate and the binding affinity of phosphate of each PS, the Michaelis-Menten constant (K_m), which was defined as the SRP concentration at equilibrium at half of the maximum binding capacity (Q_m), was calculated by Michaelis-Menten kinetics Eq. (3) (Mosier and Ladisch, 2009):

$$Q_e = \frac{Q_m C_e}{K_m + C_e} \quad (3)$$

The Freundlich model is expressed in Eq. (4), K_F and n were the Freundlich constants, the Freundlich isotherm does not yield a maximum SRP binding capacity according to Eq. (4) (Qiu et al., 2012):

$$lnQ_e = \frac{lnC_e}{n} + lnK_F \quad (4)$$

To evaluate phosphate binding capacity onto the PS based on thermodynamics, enthalpy ΔH (kJ mol^{-1}) and entropy ΔS (kJ mol^{-1} K^{-1}) were calculated using the Van't Hoff Eq. (5), Plotting ln K_L versus $-\frac{1}{T}$, slope was $\frac{\Delta H}{R}$ and intercept was $\frac{\Delta S}{R}$ make it possible to calculate ΔH and ΔS, R was the gas constant (8.314 J mol^{-1} K^{-1}) and T was the water

temperature (K) (Guerra et al., 2008; Gupta and Bhattacharyya, 2012; Huang et al., 2011):

$$lnK_L = \frac{\Delta S}{R} - \frac{\Delta H}{RT} \quad (5)$$

The Gibbs free energy ΔG (kJ mol^{-1}) was calculated as Eq. (6):

$$\Delta G = \Delta H - T\Delta S \quad (6)$$

All data were expressed as the mean values of the three replicates. The maximum binding capacity at different temperatures, or pH, and the SRP desorption were compared for each product using one-way ANOVA or Kruskal–Wallis One-way Analysis of Variance on Ranks when the normality test (Shapiro–Wilk) or Equal Variance test (Brown–Forsythe) failed using the program SigmaPlot version 14.0. A Tukey or Dunn's post hoc test was performed to identify which means or medians were significantly different from each other ($p = 0.05$ level). A Wilcoxon Signed Rank Test was used to compare the difference between pH unchanged and changed in the SRP release part Phase II. SigmaPlot version 14.0 was used to fit isotherms of the phosphorus binding data using the Langmuir and Freundlich models.

3. Results

3.1. PS binding capacity and thermodynamic parameters under different temperatures

All of the three materials (LMB, AMZ and Al) showed favorable SRP binding capacity under the six different temperatures (5, 15, 20, 25, 30 and 35 °C) employed (Fig. 1). Isotherm models revealed that the r^2 from the Langmuir isotherms were higher than those obtained for the Freundlich isotherms for LMB and AMZ (Table 1). Therefore, the binding equilibrium of phosphate on LMB and AMZ can best be described with the Langmuir isotherm (Fig. 1 (a) and (b); Table 1). SRP binding capacity of LMB was significantly impacted by temperature ($H_5 = 12.53$; $p = 0.028$). The maximum SRP precipitation capacity of LMB varied between 6.3 mg P g^{-1} at 35 °C and 14 mg P g^{-1} at 30 °C. A Tukey post hoc comparison revealed that only the precipitation capacities at 30 °C and 35 °C were significantly different from each other ($p = 0.02$). Likewise, temperature affected the SRP sorption capacity of AMZ ($H_5 = 18.22$; $p = 0.003$) that varied between 4 mg P g^{-1} at 25 °C and 29.9 mg P g^{-1} at 35 °C (Table 1). A Tukey post hoc comparison showed that the adsorption capacities at 15 °C and 25 °C ($p = 0.011$), and 25 °C and 35 °C ($p = 0.002$) were significantly different from each other. Although LMB and AMZ had their maximum P binding capacity at 30 °C and 35 °C, respectively, the K_m values at these temperatures were higher than those at other temperatures, which indicates that the SRP binding affinity of LMB and AMZ was lower than at other temperatures. Also, for Al, the Langmuir model fitted better than the Freundlich isotherm, but the accuracy of fits was lower than those for LMB and AMZ (Table 1). A Kruskal-Wallis one-way ANOVA on ranks indicated that the maximum SRP adsorption capacities in the Al treatments were not different from each other at the different temperatures tested ($H_5 = 1.07$; $p = 0.96$). Measured Q_m values ranged from 205 to 251 mg P g^{-1}, with a relatively large standard deviation varying between 11 and 16% (Table 1).

The pH in the LMB and Al treatments remained rather stable during the experiment and ranged between pH 6.47–7.91 in LMB treatments and between pH 6.94–7.51 in Al treatments (Table S2). In contrast, in AMZ treatments pH had dropped from the initial pH 7 to pH 4.65–5.73.

The ΔH values calculated were −81.27 (LMB), −45.58 (AMZ) and −19.92 (Al) kJ mol^{-1}, while ΔS were −0.26, −0.18 and −0.05 kJ mol^{-1} K^{-1}, for LMB, AMZ and Al, respectively (Table 1). The ΔG ranged from −9.69 to −1.97 kJ mol^{-1} in LMB, from −7.38 to −1.01 kJ mol^{-1} in AMZ and from −5.07 to −3.47 kJ mol^{-1} in Al when the temperature rose from 5 °C to 35 °C.

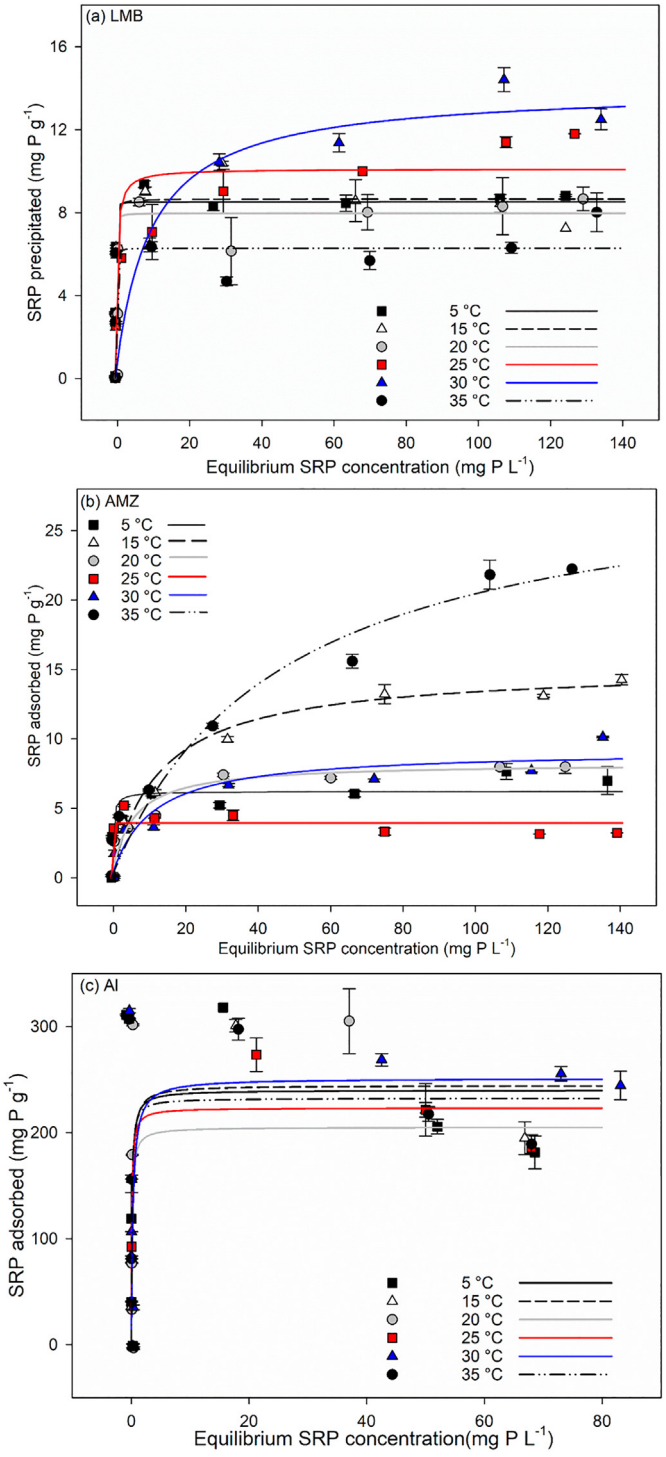

Fig. 1. SRP binding capacity for (a) LMB, (b) AMZ and (c) A1 at different temperatures (5 °C to 35 °C).The colored lines indicate the Langmuir isotherms, errors bars indicate standard deviation ($n = 3$).

3.2. Effect of pH on SRP binding capacity

The SRP binding capacities from LMB and Al were influenced by pH, while AMZ was not. For all the compounds, the highest maximum binding capacities were found at pH 6 (Table 2). The isotherm models revealed that the r^2 from the Langmuir isotherms were higher than those obtained for the Freundlich isotherms for LMB (Table 2). LMB had the highest binding capacity at pH 6 (10 mg P g^{-1}), the SRP binding capacity of LMB decreased gradually with increasing pH. The SRP

Table 1
Maximum SRP binding capacity (Q_m), estimated parameters for phosphorus binding at different temperatures of each PS using Langmuir isotherm and Freundlich adsorption isotherms.

Material	Temperature		Q_m (mg P g^{-1})	Langmuir isotherm					Freundlich isotherm			Thermodynamic		
				r^2	*p*-Value	t-Value	K_L (mg P L^{-1})	K_m (mg P L^{-1})	r^2	K_F	n^{-1}	ΔH (kJ mol^{-1})	ΔS (kJ mol^{-1} K^{-1})	ΔG (kJ mol^{-1})
LMB	5 °C	278 K	8.5 (0.2)	0.96	<0.0001	53.07	50 (0.01)	0.02 (0.01)	0.69	1.80 (0.19)	0.10 (0.05)	−81.27	−0.26	−9.69
	15 °C	288 K	8.7 (0.3)	0.91	<0.0001	35.29	20 (0.01)	0.05 (0.01)	0.65	1.78 (0.23)	0.09 (0.06)			−7.12
	20 °C	293 K	8 (0.3)	0.85	<0.0001	26.88	33.33 (0.01)	0.03 (0.01)	0.72	1.75 (0.16)	0.08 (0.04)			−5.83
	25 °C	298 K	10.1 (0.4)	0.86	<0.0001	24.13	2.63 (0.01)	0.38 (0.10)	0.61	1.59 (0.31)	0.17 (0.09)			−4.54
	30 °C	303 K	14 (1.2)	0.75	<0.0001	11.54	0.10 (0.01)	9.98 (4.53)	0.63	1.65 (0.30)	0.19 (0.08)			−3.25
	35 °C	308 K	6.3 (0.3)	0.78	<0.0001	21.31	33.33 (0.01)	0.03 (0.01)	0.53	1.56 (0.28)	0.07 (0.07)			−1.97
AMZ	5 °C	278 K	6.2 (0.3)	0.83	<0.0001	25.03	3.23 (0.12)	0.31 (0.12)	0.84	1.31 (0.14)	0.13 (0.04)	−45.58	−0.18	−7.38
	15 °C	288 K	15.2 (0.7)	0.95	<0.0001	22.98	0.07 (2.66)	13.98 (2.66)	0.80	1.38 (0.20)	0.25 (0.05)			−5.26
	20 °C	293 K	8.0 (0.4)	0.88	<0.0001	20.23	0.17 (1.57)	5.98 (1.57)	0.61	1.18 (0.33)	0.19 (0.09)			−4.19
	25 °C	298 K	4.0 (0.2)	0.77	<0.0001	23.45	106.38 (0.01)	0.01 (0.01)	0.55	1.41 (0.26)	−0.03 (0.07)			−3.13
	30 °C	303 K	9.2 (0.6)	0.88	<0.0001	16.28	0.09 (3.19)	11.29 (3.19)	0.73	0.08 (0.20)	0.47 (0.06)			−2.07
	35 °C	308 K	29.9 (2.6)	0.95	<0.0001	11.71	0.02 (11.08)	49.04 (11.08)	0.78	1.46 (0.23)	0.30 (0.07)			−1.01
Al	5 °C	278 K	239 (28.7)	0.37	<0.0001	8.35	7.84 (11.2)	0.13 (0.09)	0.14	103.02 (1.35)	0.17 (0.08)	−19.92	−0.05	−5.07
	15 °C	288 K	244.5 (27.1)	0.44	<0.0001	9.03	6.49 (12.03)	0.15 (0.08)	0.15	94.15 (1.39)	0.20 (0.10)			−4.54
	20 °C	293 K	205.2 (32.9)	0.19	<0.0001	6.24	8.46 (12.28)	0.11 (0.08)	0.16	130.11 (1.17)	0.11 (0.05)			−4.27
	25 °C	298 K	223.5 (28.1)	0.33	<0.0001	7.95	10.6 (18.24)	0.09 (0.05)	0.14	93.13 (1.38)	0.19 (0.10)			−4.00
	30 °C	303 K	251.1 (33.6)	0.29	<0.0001	7.47	3.50 (6.02)	0.28 (0.16)	0.20	85.71 (1.36)	0.21 (0.09)			−3.73
	35 °C	308 K	232.4 (28.5)	0.34	<0.0001	8.14	10.4 (19.01)	0.09 (0.05)	0.18	97.38 (1.34)	0.19 (0.09)			−3.47

Note: Q_m is the P maximum binding capacity calculated via Langmuir isotherm; K_L is the Langmuir constant, K_m is Michaelis-Menten constant; K_F is Freundlich isotherm constant; n is an empirical constant; Values inside brackets are the standard error (SE); ΔH is apparent heat of sorption; ΔS is entropy change; ΔG is the change of Gibbs free energy.

precipitation capacity of LMB at pH 10 was about 2 times lower than at pH 6 ($H_4 = 29.27$; $p < 0.001$) (Fig. 2 (a); Table 2). Both the Langmuir isotherm and the Freundlich isotherm fitted well the SRP binding data for AMZ. The SRP binding capacities of AMZ were similar from pH 6 to pH 10 ($H_4 = 9.98$; $p > 0.05$), the maximum binding capacity reached up to 7.6 mg P g^{-1} at pH 6 (Fig. 2 (b); Table 2). Nonetheless, a decrease of 30% was observed at pH 9 (5.3 mg P g^{-1}) compared to pH 6.

Similar to LMB, for Al, the r^2 from the Langmuir isotherms were higher than those from Freundlich isotherms, although the r^2 was still low (0.03 to 0.78). The highest binding capacity was found at pH 6 (572 mg P g^{-1}) (Table 2). The SRP binding capacity dropped sharply with increasing pH (Fig. 2 (c)). Kruskal-Wallis one-way ANOVA on Ranks indicated significant differences ($H_4 = 35.18$; $p < 0.001$) and a Tukey post hoc test revealed that the SRP binding capacity at pH 6 was significantly higher than the SRP binding at pH 10.

At the end of the experiment, the pH values measured in the LMB treatments ranged from pH 6.86 to pH 9.54 (Table S3). In the AMZ treatments pH values were reduced compared to the initial pH values, and they ranged from pH 5.28 to pH 7.59, while pH values in the Al treatments had remained rather stable, ranging from pH 6.98 to pH 10.04 (Table S3).

3.3. Effect of pH on phosphate release

In Phase I, the Langmuir isotherm fitted slightly better than the Freundlich isotherm (Table 3). LMB was able to precipitate 9.4 mg P g^{-1} in Phase I at pH 7. In Phase II (release phase), LMB showed a slight increase in its binding capacity from 9.4 to 10.6 mg P g^{-1} in the series with unchanged pH 7, but this difference was not significant ($H_2 = 0.05$; $p = 0.98$). In the series in which pH was changed from pH 7 to pH 10, the performance of LMB increased less; from 9.4 mg P g^{-1} in Phase I to 9.7 mg P g^{-1} in Phase II (Table 3; Fig. 3 (a)). K_m was lowest in Phase I and largest in Phase II in the series with elevated pH (Table 3). Wilcoxon Signed Rank Test revealed no difference between LMB binding capacity in Phase I and II (*Z*-Statistic (based on positive ranks) = −1.568; $p = 0.121$).

AMZ adsorbed 8.8 mg P g^{-1} in Phase I of the adsorption experiment at pH 7. In Phase II, in the series with unchanged pH (pH 7) the SRP adsorption capacity of AMZ was somewhat reduced to 7.7 mg P g^{-1} (Fig. 3 (b); Table 3). When pH was raised to pH 10, AMZ adsorption capacity significantly decreased to 5.4 mg P g^{-1} ($H_2 = 6.36$; $p = 0.042$) (Fig.3 (b)). A Dunn's Method test revealed that the adsorption capacities significantly differed between phase I and II when pH was changed ($p = 0.037$).

Table 2
Estimated parameters for SRP binding at different pH of each PS using Langmuir isotherm and Freundlich isotherms. Q_m is the SRP bind maximum in Langmuir isotherm; K_m is Michaelis-Menten constant; K_F is Freundlich isotherm constant; n is an empirical constant; Values inside brackets are the standard error (SE).

Material	pH	Q_m (mg P g^{-1})	Langmuir isotherm					Freundlich isotherm		
			r^2	*p*-Value	t-Value	K_L (mg P L^{-1})	K_m (mg P L^{-1})	r^2	K_F	n^{-1}
LMB	6	10.0 (0.4)	0.86	<0.0001	26.91	3.57 (14.93)	0.28 (0.07)	0.71	4.90 (0.05)	0.11 (0.02)
	7	9.0 (0.3)	0.80	<0.0001	23.11	1.27 (3.45)	0.79 (0.29)	0.001	3.82 (0.07)	0.02(0.02)
	8	8.8 (0.6)	078	<0.0001	15.71	0.23 (0.57)	4.28 (1.74)	0.001	3.32 (0.06)	0.01(0.02)
	9	8.3 (1.7)	0.47	<0.0001	5.01	0.04 (0.06)	23.1 (15.41)	0.031	3.25 (0.07)	0.03 (0.02)
	10	4.9 (0.7)	0.24	<0.0001	7.57	2.44 (2.44)	0.41 (0.41)	0.28	1.27 (0.26)	0.23 (0.07)
AMZ	6	7.6 (0.4)	0.82	<0.0001	19.64	0.43 (1.15)	2.34 (0.87)	0.89	4.06 (0.04)	0.14 (0.01)
	7	6.3 (0.2)	0.85	<0.0001	25.57	1.45 (4)	0.69 (0.25)	0.94	3.46 (0.03)	0.15 (0.01)
	8	5.7 (0.2)	0.87	<0.0001	23.59	0.41(1.45)	2.44 (0.69)	0.79	2.59 (0.07)	0.18 (0.02)
	9	5.3 (0.2)	0.84	<0.0001	25.91	2 (5.56)	0.50 (0.18)	0.81	3.19 (0.05)	0.13 (0.01)
	10	6.2 (0.2)	0.90	<0.0001	25.67	0.28 (1.16)	3.63 (0.86)	0.92	2.59 (0.04)	0.19 (0.01)
Al	6	571.7 (38.7)	0.78	<0.0001	14.78	2.13 (6.25)	0.47 (0.16)	0.001	484.54 (796.32)	8.33 (0.19)
	7	205.1 (33.2)	0.15	<0.0001	6.18	8.45 (12.5)	0.12 (0.08)	0.03	8000 (3.64E+6)	−0.39 (0.1)
	8	89.2 (28.8)	0.05	0005	3.10	2.14E+09 (12.5)	4.67E-10 (0.08)	0.001	197.95 (4.35)	−0.82 (0.88)
	9	38.8 (12.5)	0.03	0.005	3.10	8.75 (2.56)	0.11 (0.39)	0.001	43.38 (1.28)	−8.33 (8.33)
	10	21.3 (12.3)	0.044	0.1	1.73	9.42 (0.92)	0.11 (1.09)	0.001	43.82 (1.28)	3.45 (3.13)

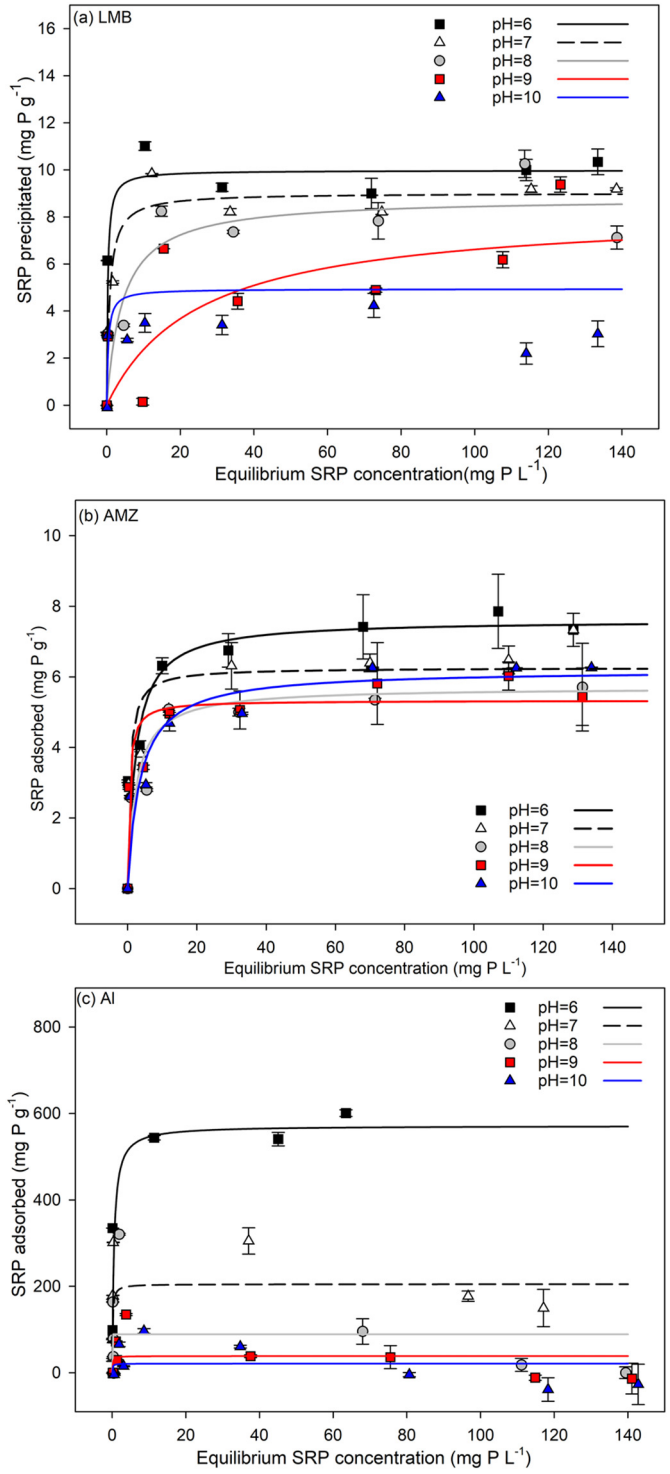

Fig. 2. The SRP maximum binding capacity of (a) LMB, (b) AMZ and (c) A1 at different pH calculated by using Langmuir isotherms (fitted lines). Error bars indicate standard deviation (n = 3).

Similarly, the binding capacity between phase II changed pH and the unchanged pH was significantly different (Z-Statistic (based on positive ranks) = −4.015; $p \le 0.001$).

Al was able to adsorb 238.3 mg P g^{-1} in Phase I at pH 7. In Phase II (release phase), Al showed a slight increase in its sorption capacity to 245.6 mg P g^{-1} in the series in which pH was not changed, but this difference was not significant ($H_2 = 12.69$; $p = 1$) (Table 3; Fig. 3 (c)). However, when pH was raised to pH 10, Al binding capacity significantly decreased to 68.3 mg P g^{-1} ($H_2 = 12.69$; $p = 0.002$). The pH changed caused a desorption of 169.9 mg P g^{-1}, resulting in a SRP concentration of about 21.5 mg P L^{-1} desorbed (Table 3). A Signed Rank Test showed a significant difference in the binding capacity between pH unchanged and pH changed to 10 in Phase II from Al (Z-Statistic (based on positive ranks) = −3.657; $p \le 0.001$).

4. Discussion

In this study, we evaluated the performance of three materials (LMB, AMZ and Al) on their SRP binding capacity at different temperatures and pH. We also compared Langmuir and Freundlich isotherms on their suitability to describe phosphorus binding capacity; and similar to other studies, we found that the Langmuir isothermal model was more suitable (Liu et al., 2016; Mucci et al., 2018; Xu et al., 2017). Therefore, our maximum binding capacity calculated for LMB, AMZ and Al under different abiotic conditions were discussed using Langmuir results.

Several studies have determined the influence of environmental factors like pH, DOC, anoxic condition and salinity on SRP binding capacity of LMB and alum (Copetti et al., 2016; Li et al., 2019; Zamparas et al., 2015). Yet, temperature, a critical environmental factor, has been studied less. In contrast to our hypothesis, warmer temperatures did not lead to more SRP being immobilized by LMB. LMB precipitated SRP in all the 6 temperatures tested without a clear pattern among the temperatures, although the maximum binding capacity dropped significantly when the temperature exceeded 30 °C (Table 1, Fig. 1 (a)). Contrary to our findings, He et al. (2017) showed that lanthanum-modified zeolite increased its P precipitation capacity from 14.8 mg g^{-1} to 17.2 mg g^{-1} when temperature increased from 20 to 40 °C. Haghseresht et al. (2009) reported that the maximum SRP binding capacity of LMB (10.5 mg g^{-1}) was reached at 35 °C, but with four runs (9.5 mg g^{-1} at 10 °C, 9.5 and 10.2 mg g^{-1} at 23 °C and 10.5 mg g^{-1} at 35 °C) no conclusions on a temperature effect can be drawn from that study. It is known that when temperature increases, the kinetic energy increases, so the particles move faster which allows higher chances of interaction between PS and SRP. However, in our experiment, we used a shaker that already increased the chances of collision between SRP and the PS, thus, the shaker could have hampered the temperature effect. As for LMB, there are hardly any articles about the influence of temperature on the adsorption performance of AMZ. The efficiency of applying AMZ at a high temperature (35 °C) was 654% higher than that at medium temperature (25 °C) and was 375% higher than that of applying LMB at the same temperature (35 °C). Although, at 35 °C it seems that the equilibrium for AMZ was not completely achieved, thus it can be that the maximum adsorption capacity for this temperature was overestimated and might never be achieved under realistic SRP concentrations. High temperatures favor the formation of monomeric and small polymeric Al (Wang et al., 2003), and thus higher SRP adsorption could be expected at warmer temperatures. Georgantas and Grigoropoulou (2007) observed increased SRP removal by Al-hydroxides with increasing temperature and attributed this to breaking of $Al(OH)_3$ polymers into smaller particles creating a larger adsorption surface. In our study, no effect of temperature on the SRP adsorption capacity of alum was observed. The use of a shaking device may have overruled more subtle temperature effects that undoubtedly will play a role in situ, where, for instance, at 5 °C the Al hydrolysis, polymerization, dispersion and floc settling will be lower than at 30 °C (Georgantas and Grigoropoulou, 2007).

Most of the PS have been applied before the growing season (winter, autumn or early spring in temperate systems) when algae have not yet taken up the SRP released from the sediment. This is largely due to the mechanism by which the modified clays works, which, different from Al salts, are not a coagulant and thus only decreases phosphate and not particulate P. However, even for Al salts, the best P adsorption results are achieved when more phosphate is available in the system because alum flocs decrease their binding capacities over time if dosed

Table 3
Estimated parameters for SRP binding capacity at different pH of each PS using Langmuir and Freundlich isotherms.

Material	Phase series		Langmuir isotherm						Freundlich isotherm		
			Q_m (mg P g^{-1})	r^2	*p*-Value	t-Value	K_m (mg SRP L^{-1})	SRP-release (μg P L^{-1})	r^2	K_F	n^{-1}
LMB	Phase I		9.4 (0.4)	0.72	<0.0001	24.43	0.06 (0.03)	<LOD	0.75	6.05 (0.04)	0.11 (0.01)
	Phase II	a (pH unchanged)	10.6 (1)	0.46	<0.0001	10.77	0.17 (0.07)	<LOD	0.30	1.22 (0.27)	0.27 (0.08)
		b (pH changed)	9.7 (0.5)	0.78	<0.0001	19.21	0.26 (0.10)	<LOD	0.67	1.71 (0.24)	0.13 (0.07)
AMZ	Phase I		8.8 (0.3)	0.85	<0.0001	25.69	6.42 (0.01)	<LOD	0.9	3.29 (0.04)	0.2 (0.01)
	Phase II	a (pH unchanged)	7.7 (0.4)	0.82	<0.0001	7.02	4.21 (1.38)	1744	0.65	1.27 (0.26)	0.16 (0.07)
		b (pH changed)	5.4 (0.3)	0.79	<0.0001	18.74	1.99 (0.71)	5504	0.58	0.93 (0.36)	0.16 (0.10)
Al	Phase I		238.3 (19.6)	0.34	<0.0001	12.17	0.11 (0.01)	<LOD	0.15	117.92 (0.20)	0.19 (0.06)
	Phase II	a (pH unchanged)	245.6 (27.1)	0.36	<0.0001	9.05	0.25 (0.11)	<LOD	0.14	106.7 (0.29)	0.22 (0.10)
		b (pH changed)	68.3 (9.7)	0.04	<0.0001	7.04	0.07 (0.06)	21,466.82	0.10	55.63 (1.11)	0.11 (0.03)

Note: Q_m is the maximum P binding capacity in Langmuir isotherm; K_m is Michaelis-Menten constant; SRP-release was calculated based on SRP concentrations difference between phase I and phase II series a or b; <LOD = below detected limit (10 μg SRP L^{-1}); K_F is Freundlich isotherm constant; n is an empirical constant; Values inside brackets are the standard error (SE).

when little or no phosphate is available (Berkowitz et al., 2006; de Vicente et al., 2008). This factor seems to be more important for efficiency than temperature; however, additional studies will be needed to develop a complete picture.

The ΔH during the SRP binding of three materials was −81.27 kJ mol^{-1}, −45.85 kJ mol^{-1} and -19.92 kJ mol^{-1} (Table 1), suggesting that the binding of phosphate onto PS was exothermic. Yet, there appeared to be no clear pattern in the SRP binding capacity of the three PS for temperature. It might be that also the use of a shaker in our study, overruled a temperature effect. As in our study, Qian et al. (2017) did not find increased phosphate removal at warmer temperatures using boehmite (a γ-AlO(OH)) mineral) as PS. $\Delta S < 0$ showed that the randomness at the solid-liquid interface decreases during the binding process. The calculated enthalpy ΔH and entropy change ΔS on the three products were negative, which indicated that the binding process was enthalpy-driven rather than entropy-driven, since only the negative sign of ΔH (but not the negative sign of ΔS) leads to the reaction being favorable (Adamson and Gast, 1967). In addition, the ΔG for LMB (−9.69 ~ −1.97 kJ mol^{-1}), AMZ (−7.38 ~ −1.01 kJ mol^{-1}) and Al (−5.07 ~ −3.47 kJ mol^{-1}) were negative, which demonstrated a spontaneous process whereby the binding force was sufficient to pass the energy barrier required for the reaction between the adsorbent and the adsorbate (Liu et al., 2011).

In agreement with our hypothesis, we found that at the highest pH, LMB had a lower SRP binding capacity (Fig. 2 and Table 2). In several studies, SRP binding efficiency of LMB has been tested under different pH values ranging from pH 4.6 to pH 9 (e.g., Gibbs et al., 2011; Mucci et al., 2018; Noyma et al., 2016; Ross et al., 2008; Zamparas et al., 2015). The LMB maximum binding capacity (9 mg P g^{-1}) at pH 7 in our study was higher than reported by Ross et al. (2008), who found 4.36 mg P g^{-1}, however, it was similar to values (10–12.3 mg P g^{-1}) reported in other studies (Haghseresht et al., 2009; Zamparas et al., 2015; Noyma et al., 2016; Mucci et al., 2018). Importantly, few studies have investigated the precipitation capacity at pH 10. In our study, LMB still could precipitate SRP at pH 10, although the maximum precipitation capacity was reduced by 50% compared to pH 6. The reduced removal capacity at pH 10 is a result of competition with hydroxyl ions for binding sites. Similar observations have been made for SRP removal by lanthanum-modified copper tailings (Jin et al., 2021). Li et al. (2019) also observed lower LMB efficiency at higher pH, with a 30% reduction in efficiency at pH 9 and a reduction of 80% at pH 10. It can, however, be expected that the hindrance by hydroxyl ions will only cause a delay in the formation of rhabdophane, but that over time most lanthanum will precipitate with phosphate. Such temporal hampering in SRP removal has also been observed in the presence of humic substances that delayed the formation of rhabdophane, but did not block it (Dithmer et al., 2016).

Similar to LMB, we found that the adsorption capacity of Al salts decreased when pH increased (Fig. 2), which is consistent with another study (Yang et al., 2006). When pH increased from 4.3 to 9.0, the P-adsorption capacity decreased from 3.5 to 0.7 mg P g^{-1} sludge (Yang et al., 2006). The addition of alum may cause the pH to drop in lakes with low alkalinity (Churchill et al., 2009), and at a low pH (below pH 5.5) and pH higher than 8, Al might occur predominantly as Al^{3+} and $Al(OH)_4^-$ (Georgantas and Grigoropoulou, 2007). These Al species are unable to adsorb phosphate, which might explain the relatively poor Langmuir fits in the experiment with pH higher than 8 ($r^2 < 0.04$). In addition, these Al species can be toxic to aquatic organisms (Yang et al., 2006). Therefore, Al salts should not be applied when the pH falls outside the safety range (6 to 8). For instance, Cooke et al. (2005) and Wagner et al. (2017) have mentioned fish kill as a result of an aluminium treatment due to pH change. In field applications, buffers such as the one we used here (sodium aluminate) are commonly applied to avoid drastic pH change and adverse consequences as fish kills (Jacoby et al., 1994; Nogaro et al., 2013). Within the safe pH range (6 to 8), alum seems to perform better at pH 6, as shown in our experiment and also by Georgantas and Grigoropoulou (2007).

Contrary to our hypothesis, AMZ did not reduce its efficiency under high pH. Our study revealed no significant difference in the SRP adsorption capacity of AMZ from the pH range pH 6 to pH 10, but the effect AMZ exerted on pH probably had a main impact on these results. The pH in our experiment had dropped from pH 9 and pH 10 at start to pH 7.2 and pH 7.6, respectively (*see* Table S3), and thus the pH lowering effect of AMZ may likely have prevented competition with hydroxyl ions. Hence, AMZ has an effect on pH (lowering it by 1.8 and 2.4 units at start pH 9 and 10), and was also found to decrease pH in sediment by 0.3–0.5 pH units (Vopel et al., 2008). In our SRP release experiment pH was elevated after 24 h of incubation compensating for acidity released from AMZ and effects of elevated pH became prominent. Few other studies have investigated the influence of pH on the maximum SRP adsorption capacities of AMZ. For instance, one study reported an AMZ adsorption of 21.5 mg of P g^{-1} in lake water with pH 6 and 7, which was reduced to 11.6 mg P g^{-1} at pH 8.9 (Gibbs et al., 2011), while another study found adsorption capacities between 4.3 and 7.6 mg of P g^{-1} in the pH range from pH 6 to pH 9 without any clear relation between its adsorption capacity and pH (Mucci et al., 2018).

There is less information on the effects of environmental factors on AMZ ability to remove phosphate than for LMB and Al. AMZ has also been used only occasionally in field applications, except for some trials in New Zealand, AMZ has not yet been applied in whole lake restoration projects (Gibbs and Hickey, 2018; Tempero and Paul, 2015). Nonetheless, AMZ has great potential for phosphorus removal in the water column and in reducing the SRP release from the sediment (Li et al., 2017; Mucci et al., 2018), and in lowering ammonium release (Gibbs and Özkundakci, 2011), while no adeverse effects on freshwater fish, crayfish, or mussels have been found (Clearwater et al., 2014). However, more information about AMZ efficacy at high pH is required as well as potential the release of Al from the zeolite matrix under such conditions.

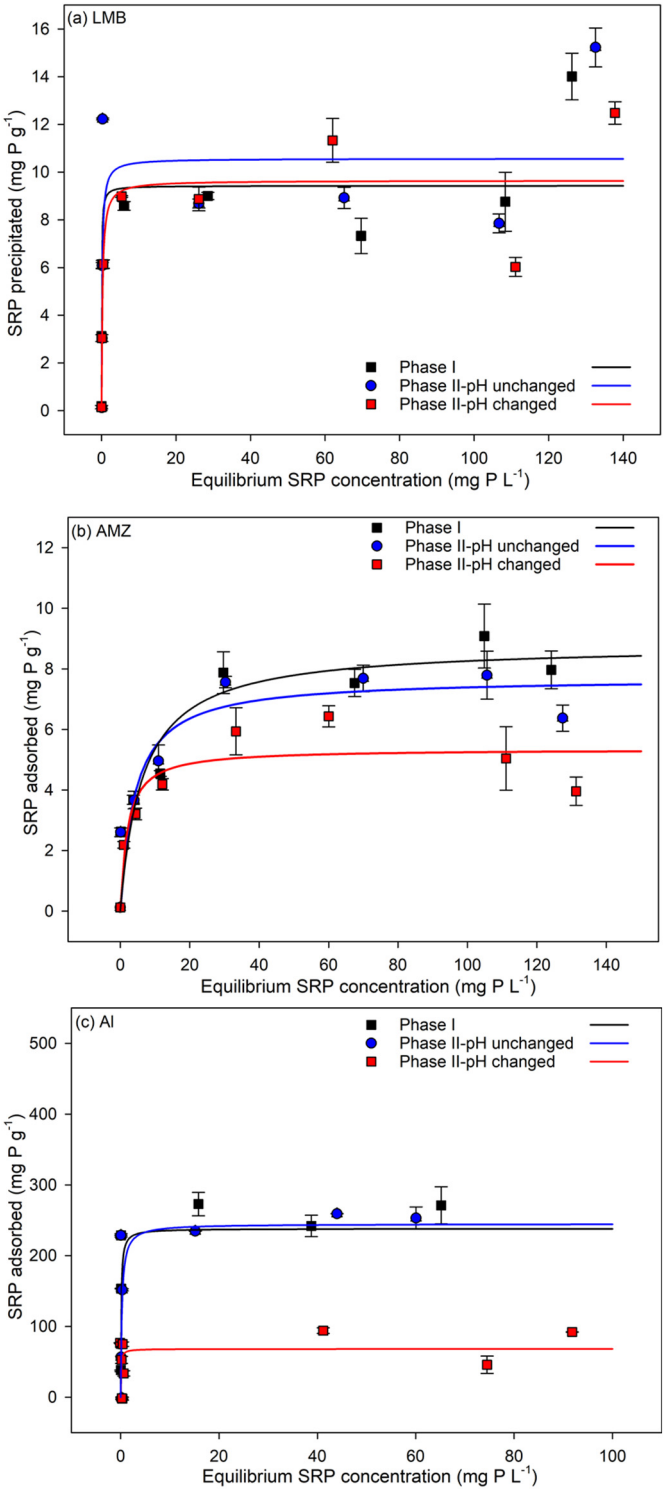

Fig. 3. Effect of changes in pH on the SRP release of (a) LMB, (b) AMZ and (c) A1. Phase I is the result at pH 7 after shaking 24 h; Phase II-pH unchanged is the result for keeping pH = 7 after shaking 48 h; Phase II-pH changed is the result of adjusting pH to 10 after shaking 48 h. Error bars indicate standard deviation (n = 3).

Contrary to our hypothesis not all of the products tested released P at higher pH (pH 10) (Fig. 3; Table 3). When pH changed from 7 to 10, AMZ desorbed approximately 39% of its adsorbed P, and alum desorbed approximately 71% of adsorbed P, while there was no release from LMB. Oppositely, LMB slightly improved its precipitation capacity when pH was changed to 10 (Phase II); however, this improvement was less than in incubations kept at pH 7, demonstrating ongoing SRP binding but also competition with hydroxyl ions as mentioned before. The higher SRP binding capacity in Phase II compared to Phase I at unchanged pH is caused by the contact time; in Phase I, LMB was in contact with SRP for 24 h, while at the end of Phase II the contact time was 48 h. Once the active ingredient of LMB, La precipitates with phosphate, it forms minerals with low solubility (i.e. rabdophane and monazite), which will not be solubilized at pH 10 (Firsching and Brune, 1991).

Differently from LMB, Al does not bind phosphate via precipitation, but via adsorption (Fig. S1); thus the SRP release at pH 10 in AMZ and Al treatments is likely a result of the higher solubility and thus the dissolution of amorphous $Al(OH)_3$. Hence, Al salts and AMZ should be avoided in shallow lakes where pH can go up to pH 10. This has been mentioned by Reitzel et al. (2013) about aluminium salts, but for AMZ, such a study has never been done. AMZ differs from alum in physical and chemical properties, with higher density and lower weight-specific P binding capacity (Clearwater et al., 2014). In AMZ the added aluminium is in the form of poly-aluminium chloride, which would suggest the phosphate removal mechanism to be similar to that of alum. Although our results indicated a relatively lower impact of elevated pH on AMZ than on Al, the earlier mentioned effect AMZ had on lowering pH seems a plausible confounding factor that warrants further investigation. In alum, the binding capacity not only decreases with pH, but also with the aging of the formed aluminium hydroxide flocs (Berkowitz et al., 2006; De Vicente et al., 2008). For instance, Berkowitz et al. (2006) found for alum added to Big Bear Lake water that the maximum sorption capacities decreased with increasing alum floc age, a maximum binding capacity of 30 mg P g^{-1} $Al(OH)_3$ for freshly-formed, amorphous material to about 15 mg P g^{-1} $Al(OH)_3$ after 180 days. If an aging effect will occur in AMZ needs to be determined.

The K_m value provides insights into the speed of the reaction between PS and SRP, while also considering the amount of saturation required (Mosier and Ladisch, 2009). A lower K_m value indicates that the PS requires only a small amount of phosphate to reach its maximum binding capacity, while a higher K_m value indicates that a higher concentration is required (Mucci et al., 2018). In this study, the overall K_m value of LMB and Al was lower than that of AMZ in all conditions, which means LMB and Al needed lower phosphate concentrations to achieve their maximum binding capacity than AMZ, suggesting better performance under realistic phosphate concentrations (Tables 1 and 2). Although the binding capacity of LMB and AMZ was the largest at 30 °C and 35 °C, respectively, both of the reaction rates were the slowest, which means that a high concentration of phosphate was required to reach the maximum binding capacity at these temperatures.

In recent decades, the need for cost-effective and eco-friendly PS has increased to mitigate eutrophication nuisance via in-lake reduction of SRP and lowering the internal P load. These materials will be considered based on safety, costs, availability and efficacy (Douglas et al., 2016; Lürling et al., 2020; Lürling et al., 2016). All three compounds tested are capable of reducing the SRP concentration in water, yet only two of them (LMB and Al) have been applied widely in hundreds of water bodies up to now (e.g. Copetti et al., 2016; Huser et al., 2016). Inasmuch as AMZ will settle to the sediment rapidly, AMZ might be an alternative for sediment injection with Al salts (Schütz et al., 2017). From a safety perspective, a large number of studies have shown that LMB is not toxic to non-target organisms (Copetti et al., 2016; Van Oosterhout and Lürling, 2011; Waajen et al., 2016). The active ingredient in LMB (lanthanum) was elevated after LMB applications in macrofauna and (cray) fish, but no detrimental effects were noted (van Oosterhout et al., 2014; Waajen et al., 2016). Hence, LMB is a powerful PS to be used in lakes that suffer from internal load issues. Likewise, laboratory assays revealed that AMZ has no side effect on the survival or growth of crayfish, mussels or fish (Clearwater et al., 2014). Thus, AMZ may also be a good candidate for P control in surface water that experiences a strong impact from internal P load.

Given that AMZ is based on a zeolite, simultaneous reduction of SRP and ammonium release of sediments could be achieved (Gibbs and Özkundakci, 2011), which may attract the attention of water quality managers. These two solid phase P sorbents may be an alternative to aluminium salts in reducing sediment P release, mainly in places where aluminium addition is prohibited. However, Al salts also have coagulating properties, and therewith water column clearing potential besides being cheaper than AMZ and LMB (Lürling et al., 2020). Overall, which compound or combination of compounds will be most suited will follow from a proper diagnosis of the problem, taking into account not only policy, cost, safety, availability, and efficacy, but also abiotic factors such as pH.

5. Conclusion

Lanthanum-modified bentonite (LMB), aluminium modified zeolite (AMZ) and aluminium salts (Al) all showed good SRP binding capacities at different temperatures and pH. Langmuir isotherm model provided better fits than Freundlich isotherm model; LMB reached its maximum binding capacity at relatively low phosphate concentrations compared to AMZ and Al; the adsorption of phosphate onto PS was exothermic. LMB and Al did not show any clear pattern in their binding capacity at different temperatures, AMZ seems to perform better at 35 °C. All the three products performed better at pH 6, while AMZ efficiency was not affected by an increase in pH, LMB and Al decreased their efficiency under high pH. AMZ and Al desorbed P when pH changed to 10, while LMB was not affected. Therefore, pH and temperature have different effects on each PS material. Abiotic factors, specifical pH, should be taken into consideration while defining the most suitable PS.

CRediT authorship contribution statement

Li Kang: Data curation, Methodology, Investigation, Writing – original draft, Writing – review & editing. **Maíra Mucci:** Conceptualization, Methodology, Supervision, Writing – review & editing. **Miquel Lürling:** Conceptualization, Resources, Supervision, Writing – review & editing.

Declaration of competing interest

The authors declare that they have no known competing financial interests or personal relationships that could have appeared to influence the work reported in this paper.

Acknowledgment

We thank Wendy Beekman and Frits Gillissen from Wageningen University for their assistance, we also sincerely thank the two reviewers for their constructive suggestions. Li Kang was sponsored by a CSC Grant, China (No. 201906050134).

Appendix A. Supplementary data

Supplementary data to this article can be found online at https://doi.org/10.1016/j.scitotenv.2021.151489.

References

Adamson, A.W., Gast, A.P., 1967. Physical Chemistry of Surfaces. vol. 150. Interscience publishers, New York.

Berkowitz, J., Anderson, M.A., Amrhein, C., 2006. Influence of aging on phosphorus sorption to alum floc in lake water. Water Res. 40, 911–916.

Busca, G., 2014. Zeolites and other structurally microporous solids as acid-base materials. Heterog. Catal. Mater. 197–249.

Churchill, J.J., Beutel, M.W., Burgoon, P.S., 2009. Evaluation of optimal dose and mixing regime for alum treatment of Matthiesen Creek inflow to Jameson Lake, Washington. Lake Reserv. Manag. 25, 102–110.

Clearwater, S.J., Hickey, C.W., Thompson, K.J., 2014. The effect of chronic exposure to phosphorus-inactivation agents on freshwater biota. Hydrobiologia 728, 51–65.

Cooke, G.D., Welch, E.B., Peterson, S., Nichols, S.A., 2005. Restoration and Management of Lakes and Reservoirs. CRC Press.

Copetti, D., Finsterle, K., Marziali, L., Stefani, F., Tartari, G., Douglas, G., et al., 2016. Eutrophication management in surface waters using lanthanum modified bentonite: a review. Water Research 97, 162–174.

De Vicente, I., Huang, P., Andersen, F.Ø., Jensen, H.S., 2008. Phosphate adsorption by fresh and aged aluminum hydroxide. Consequences for lake restoration. Environ.Sci. Technol. 42, 6650–6655.

Dionisio, K.L., Phillips, K., Price, P.S., Grulke, C.M., Williams, A., Biryol, D., et al., 2018. The chemical and products database, a resource for exposure-relevant data on chemicals in consumer products. Sci.Data 5, 180125.

Dithmer, L., Nielsen, U.G., Lundberg, D., Reitzel, K., 2016. Influence of dissolved organic carbon on the efficiency of P sequestration by a lanthanum modified clay. Water Res. 97, 39–46.

Douglas, 2002 GB Douglas Remediation material and remediation process for sediments. Google Patents, 2002.

Douglas, G.B., Lurling, M., Spears, B.M., 2016. Assessment of changes in potential nutrient limitation in an impounded river after application of lanthanum-modified bentonite. Water Res. 97, 47–54.

Du, C., Ren, X., Zhang, L., Xu, M., Wang, X., Zhuang, Y., et al., 2016. Adsorption characteristics of phosphorus onto soils from water level fluctuation zones of the Danjiangkou Reservoir. CLEAN–Soil Air Water 44, 975–983.

Fastner, J., Abella, S., Litt, A., Morabito, G., Vörös, L., Pálffy, K., et al., 2016. Combating cyanobacterial proliferation by avoiding or treating inflows with high P load—experiences from eight case studies. Aquat. Ecol. 50, 367–383.

Firsching, F.H., Brune, S.N., 1991. Solubility products of the trivalent rare-earth phosphates. J.Chem.Eng.Data 36, 93–95.

Fraters, B., AEJ, Hooijboer, GBJ, Rijs, van Duijnhoven, N., Rozemeijer, J.C., 2017. Water quality in the Netherlands; status (2012-2015) and trend (1992-2015): Addendum to report 2016-0019. Waterkwaliteit in Nederland; toestand (2012-2015) en trend (1992-2015): Addendum bij rapport 2016-0019.

Georgantas, D.A., Grigoropoulou, H.P., 2007. Orthophosphate and metaphosphate ion removal from aqueous solution using alum and aluminum hydroxide. J. Colloid Interface Sci. 315, 70–79.

Gibbs, M., Özkundakci, D., 2011. Effects of a modified zeolite on P and N processes and fluxes across the lake sediment–water interface using core incubations. Hydrobiologia 661, 21–35.

Gibbs, M.M., Hickey, C.W., 2018. Flocculants and Sediment Capping for Phosphorus Management. Lake Restoration Handbook. Springer, pp. 207–265.

Gibbs, M.M., Hickey, C.W., Özkundakci, D., 2011. Sustainability assessment and comparison of efficacy of four P-inactivation agents for managing internal phosphorus loads in lakes: sediment incubations. Hydrobiologia 658, 253–275.

Guerra, D.L., Lemos, V.P., Angélica, R.S., Airoldi, C., 2008. The modified clay performance in adsorption process of Pb2+ ions from aqueous phase—thermodynamic study. Colloids Surf. A Physicochem. Eng. Asp. 322, 79–86.

Gupta, S.S., Bhattacharyya, K.G., 2012. Adsorption of heavy metals on kaolinite and montmorillonite: a review. Phys. Chem. Chem. Phys. 14, 6698–6723.

Haghseresht, F., Wang, S., Do, D.D., 2009. A novel lanthanum-modified bentonite, phoslock, for phosphate removal from wastewaters. Appl. Clay Sci. 46 (4), 369–375.

Hamilton, D.P., Salmaso, N., Paerl, H.W., 2016. Mitigating harmful cyanobacterial blooms: strategies for control of nitrogen and phosphorus loads. Aquat. Ecol. 50, 351–366.

He, Y., Lin, H., Dong, Y., Wang, L., 2017. Preferable adsorption of phosphate using lanthanum-incorporated porous zeolite: characteristics and mechanism. Appl. Surf. Sci. 426, 995–1004.

Hebbar, R.S., Isloor, A.M., Ismail, A.F., 2014. Preparation and evaluation of heavy metal rejection properties of polyetherimide/porous activated bentonite clay nanocomposite membrane. RSC Adv. 4, 47240–47248.

Huang, L., Fu, L., Jin, C., Gielen, G., Lin, X., Wang, H., et al., 2011. Effect of temperature on phosphorus sorption to sediments from shallow eutrophic lakes. Ecol. Eng. 37, 1515–1522.

Huser, B.J., Futter, M., Lee, J.T., Perniel, M., 2016. In-lake measures for phosphorus control: the most feasible and cost-effective solution for long-term management of water quality in urban lakes. Water Res. 97, 142–152.

Jacoby, J.M., Gibbons, H.L., Stoops, K.B., Bouchard, D.D., 1994. Response of a shallow, polymictic lake to buffered alum treatment. Lake Reserv. Manag. 10, 103–112.

Jalali, M., Peikam, E.N., 2013. Phosphorus sorption–desorption behaviour of river bed sediments in the Abshineh river, Hamedan, Iran, related to their composition. Environ. Monit. Assess. 185, 537–552.

Jeppesen, E., Kronvang, B., Meerhoff, M., Sondergaard, M., Hansen, K.M., Andersen, H.E., et al., 2009. Climate change effects on runoff, catchment phosphorus loading and lake ecological state, and potential adaptations. J. Environ. Qual. 38, 1930–1941.

Jin, H., Lin, L., Meng, X., Wang, L., Huang, Z., Liu, M., et al., 2021. A novel lanthanum-modified copper tailings adsorbent for phosphate removal from water. Chemosphere 281, 130779.

Jin, X., Xu, Q., Huang, C., 2005. Current status and future tendency of lake eutrophication in China. Sci. China C Life Sci. 48.

Johannesson, K.H., Lyons, W.B., 1994. The rare earth element geochemistry of mono lake water and the importance of carbonate complexing. Limnol. Oceanogr. 39 (5), 1141–1154.

Kragh, T., Sand-Jensen, K., 2018. Carbon limitation of lake productivity. Proc. R. Soc. B 285, 20181415.

Langmuir, I., 1918. The adsorption of gases on plane surfaces of glass, mica and platinum. J. Am. Chem. Soc. 40, 1361–1403.

Li, X., Zhang, Z., Xie, Q., Yang, R., Guan, T., Wu, D., 2019. Immobilization and release behavior of phosphorus on phoslock-inactivated sediment under conditions simulating the photic zone in eutrophic Shallow Lakes. Environ. Sci. Technol. 53, 12449–12457.

Li, Y., Fan, Y., Li, X., Wu, D., 2017. Evaluation of zeolite/hydrous aluminum oxide as a sediment capping agent to reduce nutrients level in a pond. Ecol. Eng. 101, 170–178.
Liu, J., Wan, L., Zhang, L., Zhou, Q., 2011. Effect of pH, ionic strength, and temperature on the phosphate adsorption onto lanthanum-doped activated carbon fiber. J. Colloid Interface Sci. 364, 490–496.
Liu, S., Li, J., Yang, Y., Wang, J., Ding, H., 2016. Influence of environmental factors on the phosphorus adsorption of lanthanum-modified bentonite in eutrophic water and sediment. Environ. Sci. Pollut. Res. 23, 2487–2494.
Lürling, M., Smolders, A.J.P., Douglas, D., 2020. Internal phosphorus loading of lakes: Causes, case Studies, and management. Chapter 5: Methods for the management of internal loading. J. Ross Publishing, pp. 77–107.
Lürling, M., van Oosterhout, F., 2013. Controlling eutrophication by combined bloom precipitation and sediment phosphorus inactivation. Water Res. 47, 6527–6537.
Lürling, M., Waajen, G., van Oosterhout, F., 2014. Humic substances interfere with phosphate removal by lanthanum modified clay in controlling eutrophication. Water Res. 54, 78–88.
Lürling, M., Mackay, E., Reitzel, K., Spears, B.M., 2016. Editorial–A Critical Perspective on Geo-engineering for Eutrophication Management in Lakes. Elsevier.
Lürling, M., Kang, L., Mucci, M., van Oosterhout, F., Noyma, N.P., Miranda, M., et al., 2020. Coagulation and precipitation of cyanobacterial blooms. Ecol. Eng. 158, 106032.
Mosier, N.S., Ladisch, M.R., 2009. Modern Biotechnology. Wiley Online Library.
Mucci, M., Maliaka, V., Noyma, N., Marinho, M., Lurling, M., 2018. Assessment of possible solid-phase phosphate sorbents to mitigate eutrophication: influence of pH and anoxia. Sci. Total Environ. 619, 1431–1440.
NNI, 1986. Water–Photometric Determination of the Content of Dissolved Orthophosphate and the Total Content of Phosphorous Compounds by Continuous Flow Analysis.
Nogaro, G., Burgin, A.J., Schoepfer, V.A., Konkler, M.J., Bowman, K.L., Hammerschmidt, C.R., 2013. Aluminum sulfate (alum) application interactions with coupled metal and nutrient cycling in a hypereutrophic lake ecosystem. Environ. Pollut. 176, 267–274.
Noyma, N.P., de Magalhães, L., Furtado, L.L., Mucci, M., van Oosterhout, F., Huszar, V.L.M., et al., 2016. Controlling cyanobacterial blooms through effective flocculation and sedimentation with combined use of flocculants and phosphorus adsorbing natural soil and modified clay. Water Res. 97, 26–38.
OECD, 2017. Diffuse Pollution, Degraded Waters.
Paerl, H.W., 2014. Mitigating harmful cyanobacterial blooms in a human- and climatically-impacted world. Life 4, 988–1012.
Paerl, H.W., Paul, V.J., 2012. Climate change: links to global expansion of harmful cyanobacteria. Water Res. 46, 1349–1363.
Paerl, H.W., Gardner, W.S., Havens, K.E., Joyner, A.R., McCarthy, M.J., Newell, S.E., et al., 2016. Mitigating cyanobacterial harmful algal blooms in aquatic ecosystems impacted by climate change and anthropogenic nutrients. Harmful Algae 54, 213–222.
Poikane, S., Kelly, M.G., Herrero, F.S., Pitt, J.A., Jarvie, H.P., Claussen, U., et al., 2019. Nutrient criteria for surface waters under the European Water Framework Directive: current state-of-the-art, challenges and future outlook. Sci. Total Environ. 695, 14.
Qian, J., Shen, M., Wang, P., Wang, C., Hu, J., Hou, J., et al., 2017. Co-adsorption of perfluorooctane sulfonate and phosphate on boehmite: influence of temperature, phosphate initial concentration and pH. Ecotoxicol. Environ. Saf. 137, 71–77.
Qiu, T., Zeng, Y., Ye, C., Tian, H., 2012. Adsorption thermodynamics and kinetics of p-xylene on activated carbon. J. Chem. Eng. Data 57, 1551–1556.
Reddy, K.R., DeLaune, R.D., 2008. Biogeochemistry of Wetlands: Science and Applications. CRC Press.
Reitzel, K., Jensen, H.S., Egemose, S., 2013. pH dependent dissolution of sediment aluminum in six danish lakes treated with aluminum. Water Res. 47 (3), 1409–1420.
Ross, C.S., Shannon, E.V., 1926. The minerals of bentonite and related clays and their physical properties. J. Am. Ceram. Soc. 9, 77–96.
Ross, G., Haghseresht, F., Cloete, T.E., 2008. The effect of pH and anoxia on the performance of Phoslock®, a phosphorus binding clay. Harmful Algae 7, 545–550.
Sanseverino, I., Conduto, D., Pozzoli, L., Dobricic, S., Lettieri, T., 2016. Algal Bloom and Its Economic Impact. European Commission, Joint Research Centre Institute for Environment and Sustainability.
Schütz, J., Rydin, E., Huser, B.J., 2017. A newly developed injection method for aluminum treatment in eutrophic lakes: effects on water quality and phosphorus binding efficiency. LakeReserv.Manag. 33, 152–162.
Smeltzer, E., Kirn, R.A., Fiske, S., 1999. Long-term water quality and biological effects of alum treatment of Lake Morey, Vermont. Lake Reserv. Manag. 15, 173–184.
Smith, V.H., Schindler, D.W., 2009. Eutrophication science: where do we go from here? Trends Ecol. Evol. 24, 201–207.
Søndergaard, M., Bjerring, R., Jeppesen, E., 2013. Persistent internal phosphorus loading during summer in shallow eutrophic lakes. Hydrobiologia 710, 95–107.
Spears, B.M., Dudley, B., Reitzel, K., Rydin, E., 2013. Geo-Engineering in Lakes A Call for Consensus. ACS Publications.
Tempero, G.W., Paul, W.J., 2015. Flocculation and sediment capping – fact sheet. Lake Ecosystem Restoration New Zealand (LERNZ). University of Waikato, Hamilton, New Zealand.
van Galen, M., Baltussen, W., Gardebroek, K., Herceglić, N., Hoste, R., Ihle, R., et al., 2020. Agro-Nutri Monitor 2020: Monitor prijsvorming voedingsmiddelen en analyse belemmeringen voor verduurzaming. Wageningen Economic Research.
van Oosterhout, F., Lürling, M., 2011. Effects of the novel 'Flock & Lock'lake restoration technique on Daphnia in Lake Rauwbraken (The Netherlands). J. Plankton Res. 33, 255–263.
van Oosterhout, F., Goitom, E., Roessink, I., Lürling, M., 2014. Lanthanum from a modified clay used in eutrophication control is bioavailable to the marbled crayfish (Procambarus fallax f. virginalis). PLoS one 9, e102410.
Vopel, K., Gibbs, M., Hickey, C.W., Quinn, J., 2008. Modification of sediment-water solute exchange by sediment capping materials: effects on O2 and pH. Mar. Freshw. Res. 59, 1101–1110.
Waajen, G., van Oosterhout, F., Douglas, G., Lürling, M., 2016. Management of eutrophication in Lake De Kuil (The Netherlands) using combined flocculant–Lanthanum modified bentonite treatment. Water Res. 97, 83–95.
Wagner, K.J., Meringolo, D., Mitchell, D.F., et al., 2017. Aluminum treatments to control internal phosphorus loading in lakes on Cape Cod, Massachusetts. Lake Reserv. Manag. 33 (2), 171–186.
Wang, S.L., Wang, M.K., Tzou, Y.M., 2003. Effect of temperatures on formation and transformation of hydrolytic aluminum in aqueous solutions. Colloids Surf. A Physicochem. Eng. Asp. 231, 143–157.
Xu, R., Zhang, M., Mortimer, R.J.G., Pan, G., 2017. Enhanced phosphorus locking by novel lanthanum/aluminum–hydroxide composite: implications for eutrophication control. Environ.Sci.Technol. 51, 3418–3425.
Yang, Y., Zhao, Y.Q., Babatunde, A.O., Wang, L., Ren, Y.X., Han, Y., 2006. Characteristics and mechanisms of phosphate adsorption on dewatered alum sludge. Sep. Purif. Technol. 51, 193–200.
Zamparas, M., Gavriil, G., Coutelieris, F.A., Zacharias, I., 2015. A theoretical and experimental study on the P-adsorption capacity of Phoslock™. Appl. Surf. Sci. 335, 147–152.